



# Development and Characterization of 3D Hybrid Spheroids for the Investigation of the Crosstalk Between B-Cell Non-Hodgkin Lymphomas and Mesenchymal Stromal Cells

Kamila Duś-Szachniewicz <sup>1</sup>, Katarzyna Gdesz-Birula<sup>1</sup>, Grzegorz Rymkiewicz <sup>2</sup>

<sup>1</sup>Institute of General and Experimental Pathology, Department of Clinical and Experimental Pathology, Wrocław Medical University, Wrocław, Poland;

<sup>2</sup>Flow Cytometry Laboratory, Department of Cancer Pathomorphology, Maria Skłodowska-Curie National Research Institute of Oncology, Warsaw, Poland

Correspondence: Kamila Duś-Szachniewicz, Department of Clinical and Experimental Pathology, Institute of General and Experimental Pathology, Wrocław Medical University, Marcinkowskiego 1, Wrocław, 50-368, Poland, Tel +48 71 7871212, Email kamila.dus-szachniewicz@umw.edu.pl

**Purpose:** B-cell non-Hodgkin lymphomas (B-NHLs) are the most common lymphoproliferative malignancy. Despite targeted therapies, the bone marrow involvement remains a challenge in treating aggressive B-NHLs, partly due to the protective interactions of lymphoma cells with mesenchymal stromal cells (MSCs). However, data elucidating the relationship between MSCs and B-NHLs are limited and inconclusive due to the lack of reproducible in vitro three-dimensional (3D) models. Here, we developed and described a size-controlled and stable 3D hybrid spheroids of Ri-1 (diffuse large B-cell lymphoma, DLBCL) and RAJI (Burkitt lymphoma, BL) cells with HS-5 fibroblasts to facilitate research on the crosstalk between B-NHL cells and MSCs.

**Materials and Methods:** We applied the commercially available agarose hydrogel microwells for a fast, low-cost, and reproducible hybrid lymphoma/stromal spheroids formation. Standard histological automated procedures were used for formalin fixation and paraffin embedding (FFPE) of 3D models to produce good quality slides for histopathology and immunohistochemical staining. Next, we tested the effect of the anti-cancer drugs: doxorubicin (DOX) and ibrutinib (IBR) on mono-cultured and co-cultured B-NHLs with the use of alamarBlue and live/dead cell fluorescence based assays to confirm their relevancy for drug testing studies.

**Results:** We optimized the conditions for B-NHLs spheroid formation in both: a cell line-specific and application-specific manner. Lymphoma cells aggregate into stable spheroids when co-cultured with stromal cells, of which internal architecture was driven by self-organization. Furthermore, we revealed that co-culturing of lymphoma cells with stromal cells significantly reduced IBR-induced apoptosis compared to the 3D mono-culture.

**Conclusion:** This article provides details for generating 3D B-NHL spheroids for the studies on the lymphoma- stromal cells. This approach makes it suitable to assess in a relevant in vitro model the activity of new therapeutic agents in B-NHLs.

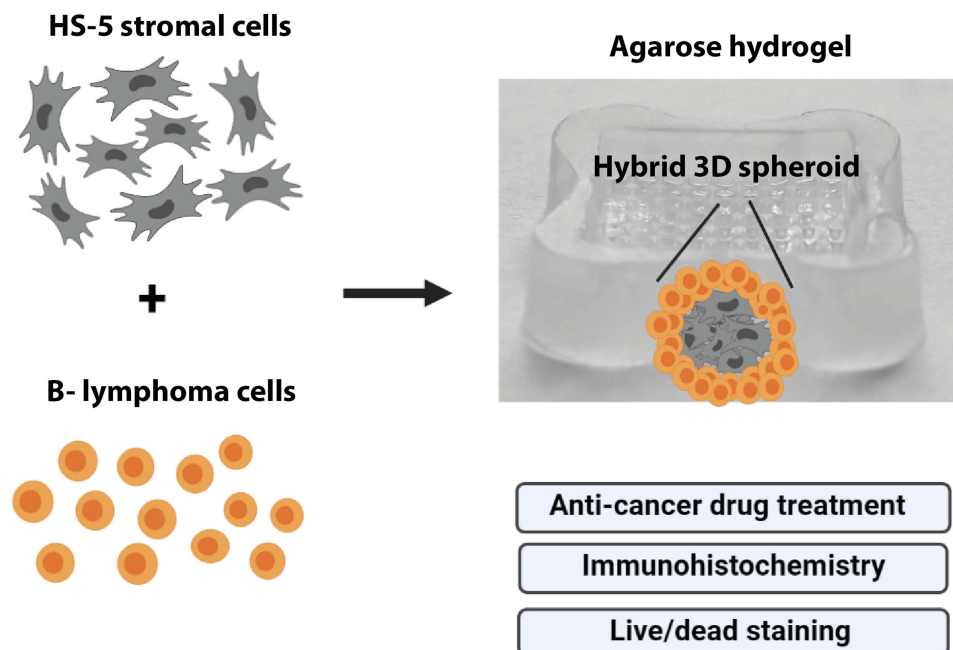
**Keywords:** 3D lymphoma model, hybrid cell spheroids, lymphoma-stromal cell crosstalk, doxorubicin, ibrutinib, agarose hydrogel microwells

## Introduction

Burkitt lymphoma (BL) and diffuse large B-cell lymphomas (DLBCL) represent heterogeneous and aggressive mature B-cell non-Hodgkin lymphomas (B-NHLs).<sup>1,2</sup> Approximately 20% and from 11 to 34% of patients with BL, and DLBCLs, respectively, have bone marrow (BM) involvement.<sup>3,4</sup> Importantly, BM involvement by DLBCLs and BL is clinically recognized as a high-risk advanced disease.<sup>5</sup>

Key components of the BM niche are non-hematopoietic multipotent cells, known as mesenchymal stromal cells (MSCs). They support and regulate hematopoietic stem/progenitor cell homeostasis,<sup>6</sup> however, not by direct contact or secretion of soluble factors.<sup>7</sup> Ongoing research demonstrates that MSCs impact tumor growth and progression.

## Graphical Abstract



Interestingly, some studies show conflicting results indicating both: antitumorigenic,<sup>8–12</sup> and protumorigenic<sup>13–18</sup> properties of MSCs, still their net effect appears to be predominantly pro-tumorigenic. Several groups reported BM stromal cells providing chemoprotection to hematopoietic tumor cells via secreted inflammatory and chemotactic cytokines, such as CXCR12, IL-6, and IL-8, from the inhibitory effect of a treatment.<sup>19–21</sup> However, direct cell–cell interactions are the ones that are essential for the chemoprotection of lymphoma cells by the bone marrow niche. Over a decade ago, Lwin et al established that BM stromal cells-derived BAFF (B cell-activating factor belonging to the TNF family) protects B-NHL cells from spontaneous apoptosis and is involved in cell adhesion-mediated drug resistance.<sup>22</sup> In turn, Mraz and co-authors established that co-cultures of rituximab-responsive B-NHL cells with HS-5 stromal cells significantly reduced rituximab-induced apoptosis compared to cells cultured on a plastic surface.<sup>20</sup> Interestingly, this experiment demonstrated that the protective effect of stromal cells on rituximab cytotoxicity was very similar in magnitude to the cell adhesion-mediated resistance to doxorubicin (DOX). The importance of cell–cell interaction in lymphoma protection against anti-cancer drugs is still unknown. It is also inconclusive whether an interaction with MSCs could lead to the emergence of chemoresistant cells at a physiologically relevant drug dose. This is partially due to the lack of reproducible models for direct studies of lymphoma-stromal cells interactions.

The development of preclinical models with more relevant translational predictivity for the response of human cancers to drug candidates garnered much attention in recent years. The traditional model for *in vitro* study and drug screening is the two-dimensional (2D) culture, which reflects neither the three-dimensional (3D) architecture nor the complex cell–cell and cell–microenvironmental interactions.<sup>23–25</sup> For those reasons, the drug testing studies with 2D models mostly fail to predict *in vivo* responses to anti-cancer treatment.<sup>26–28</sup> Concurrently, *in vitro* drug testing studies performed with 3D tumor spheroids predict the *in vivo* sensitivity of tumor cells more accurately.<sup>29–31</sup>

Spheroids aggregates can be established from a single cell type or mixtures of multiple cell types, including tumor, stromal, and immune cells. Given that tumors are composed of multiple cell types, 3D co-culturing increases the complexity of tumor models.<sup>32–34</sup> Unfortunately, there is a lack of well-characterized 3D hybrid models for studying DLBCL lymphoma- microenvironment crosstalk. Regarding DLBCL lymphomas, in 2017 a three-dimensional

lymphoma-on-chip model, recapitulating the interactions between immune cells, cancer cells, and endothelial cells in the tumor microenvironment of DLBCL, was successfully developed.<sup>35</sup> Recently, Foxall et al described a collagen scaffolds-based spheroid co-culture system comprising DLBCL cells, cancer-associated fibroblasts (CAF), and tumor-associated macrophages (TAM).<sup>36</sup> Notably, both studies demonstrated that DLBCL cells interact with their constituent components, resulting in their improved viability compared to 2D mono-cultures. Finally, An et al successfully developed a canine 3D hybrid model by co-culturing the lymphoma cells, and lymph node-derived primary stromal cells.<sup>37</sup> Importantly, they observed that lymphoma co-culture with stromal cells influenced apoptosis and the cell cycle of tumor cells, as well as upregulated multidrug resistance genes, such as *P-gp*, *MRP1*, and *BCRP*, compared with 3D mono-cultures. The above study revealed that understanding the interaction between the tumor microenvironment and lymphoma cells is essential in designing experimental approaches to personalized medicine and predicting the effects of drugs.

Unlike solid tumors, lymphoma cells grow in suspension *in vitro*. When cultured under standard 3D methods (eg, hanging drop, ultra-low attachment plates, rotary cell cultures),<sup>38</sup> lymphoma cells form relatively flat aggregates. The above methods have other limitations, such as a lack of reproducibility and variability of spheroid sizes.<sup>39,40</sup> Recently, hydrogels (water-swollen networks of polymers) have been widely used for spheroid preparation due to their biocompatibility and biodegradable properties. Moreover, hydrogel microwells provide a facile method to produce uniform-sized spheroids in a fast and low-cost manner.<sup>41,42</sup> Notably, it was observed that they mimic salient elements of native extracellular matrices, and their mechanical properties are similar to those of many soft tissues, thus they can support cell adhesion.<sup>43,44</sup>

The objective of this study was to develop and characterize over days the hybrid B-cell lymphoma/stromal cells models with the use of low-cost, fast, and commercially available hydrogel microwells. We successfully generated two co-culture systems that recapitulate the interaction of lymphoma cells with MSCs. Our 3D hybrid spheroids were prepared using two B-NHL cell lines: Ri-1 and Raji representing DLBCL and BL, respectively. First, the growth and proliferation characteristics of 3D cultures were characterized over days using an image analysis demonstrating the differences between mono-cultures and hybrid spheroids. Next, we have confirmed the suitability of the generated models for applications, such as drug screening, allowing comparison of cell growth, survival, and invasiveness between treatment conditions. Taken together, we conclude the B-NHL hybrid spheroids are a promising preclinical model for studying the mechanism of lymphoma-MSCs interactions and for screening anti-cancer drugs.

## Materials and Methods

### Cells and Cell Line Culture

The human bone marrow cells HS-5 were obtained from American Type Culture Collection (ATCC, MD, USA). The DLBCL cell line Ri-1 and BL cell line Raji were received from German Collection of Microorganisms and Cell Cultures (DSMZ, Germany). The cells were cultured in RPMI-1640 (Gibco, UK) with 10% fetal bovine serum (Gibco, UK) and 1% penicillin/streptomycin (Gibco, UK). The cells were grown at 37 °C in a humid atmosphere saturated with 5% CO<sub>2</sub>, and readjusted every week to a concentration of at least 1×10<sup>6</sup> cells/mL by dilution in fresh complete medium or into new flasks.

### Preparation of Microwells and Spheroids

Spheroids were generated using a non-adhesive agarose microwell system (mold 12–256, 3D PetriDish<sup>®</sup>, Microtissues Inc., RI, USA) according to the manufacturer's instructions. In brief, molds with 15 mm wide and 3 mm high, containing 256 micropores of 400 μm diameter each, were used to create gel microwells. A 2% agarose solution (w/v in H<sub>2</sub>O, UltraPure<sup>™</sup> Agarose, Invitrogen, Thermo Fisher Scientific, UK) was molten by microwaving, cooled to about 60 °C, and 500 μL of agarose was pipetted on top of the mold. Once the agarose gelled at room temperature, the microwell was gently separated from the mold, UV irradiated for at least 30 min and stored in PBS up to 7 days in 4 °C.

Prior to the preparation of spheroids, the agarose microwell was placed in a glass-bottom dish with a diameter of 35 mm, and was incubated for 15 minutes with the warm culture medium to equilibrate the gel. Next, the culture medium from the outside of the gel and from the cell seeding chamber was carefully removed. Cells were counted with an

automated cell counter (Thermo Fisher Scientific, Germany) and appropriate cell dilutions have been prepared. Spheroids were obtained by seeding  $3.2 \times 10^4$  cells per mold (seeding densities of 125 cells/well). Mixed spheroids were prepared from  $3.2 \times 10^4$  cells in four ratios of lymphomas to stromal cells, including 1:1, 1:2, 1:4, and 1:10. 190  $\mu$ L of cell suspension was carefully dropped into the cell seeding chamber. The cells fell to the bottom of the micropores in the gel in approximately 10 minutes, and up to 4 mL of the additional culture medium was added to the outside of the microwells gel. The medium was exchanged after 24 h and then every other 2 days. The spheroids were grown at 37 °C in a humid atmosphere saturated with 5% CO<sub>2</sub> for a maximum of 14 days. The morphology and size of spheroids were monitored every 24 h until day 14 by bright field microscopy using an inverted Olympus IX73 microscope (Olympus, Germany) with the Olympus Cell<sup>A</sup> software.

## Spheroid Dissociation and Trypan Blue Staining

At each time point, spheroids were assessed by automated counting for overall viability using the trypan blue dye exclusion method. First, the spheroids were taken up in 1 mL TrypLE Express Enzyme (Gibco, UK) and incubated in a water bath at 37 °C for 15 min for dissociation. The suspension was then homogenized by gently pipetting up and down 5–10 times with a wide borehole pipette tip, and the reaction was quenched by adding 5 mL of the culture medium. Next, a 1:1 (vol/vol) mixture of dissociated cells and 0.4% trypan blue (Merck, Germany) was incubated for 2 min at room temperature. Viability was evaluated in an automated cell counter and by the provided software (Thermo Fisher Scientific, Germany), adjusting the cell size gate between 6 and 20  $\mu$ m.

## Histological Processing and Immunohistochemistry

Entire hydrogels with multiple spheroids were fixed for 30 minutes with a 10% formalin neutral buffer solution. According to the manufacturer's instructions, the top of the hydrogel was covered by Cytoblock Replacement Reagents (Thermo Fisher Scientific, Germany) to prevent displacement of spheroids during histological processing. Entire agarose blocks underwent automated tissue processing (Thermo Fisher Scientific, Germany) and were embedded in paraffin as a final step. Five-micrometer-thick paraffin sections were prepared. Spheroids were deparaffinized, rehydrated, and stained with hematoxylin. The immunostaining was performed using a monoclonal mouse anti-human antibody against CD20 (clone L26, cat No. IS604, Dako, Denmark) on an autostainer (Autostainer Plus; Dako, Inc., Denmark) according to the manufacturer's manual.

## Live/Dead Staining of Spheroids

Cell viability was monitored by live/dead cell viability/cytotoxicity assay (Thermo Fisher Scientific, Germany) after 7 and 14 days of cell seeding. Briefly, the culture medium was removed, and spheroids in each hydrogel sample were washed three times in PBS for 5 minutes. Next, spheroids were incubated with a 200  $\mu$ L of PBS solution containing 1  $\mu$ M Calcein AM targeting living cells and 4  $\mu$ M Ethidium homodimer-1 labeling dead cells at 37 °C for 30 minutes, protected from the light, as instructed by the manual. Green and red fluorescence was detected at excitation/emission wavelengths of 485/530 and 550/590 nm, respectively, and imaged under a fluorescence microscope Olympus BX43 with the Olympus cellSens software. The green and red fluorescence intensity was separately analyzed by ImageJ software (National Institutes of Health, MD, USA), and the percentage of living and dead cells in spheroids was calculated by the corrected total cell fluorescence (CTCF) intensity.<sup>45</sup>

## AlamarBlue Assay

Doxorubicin (DOX) and ibrutinib (IBR) were purchased from Sigma-Aldrich (Steinheim am Albuch, Germany), Stock concentrations for DOX (1mM) were made in nuclease-free water and stored at -20 °C, while IBR (10 mM) was dissolved in dimethyl sulfoxide (DMSO, Sigma Aldrich) and stored at 4 °C. Working stocks were made in the culture media.

The alamarBlue assay was performed to determine the drug IC<sub>50</sub> values in B-NHL cell lines, as previously described.<sup>46</sup> Three-day co-cultures of Ri-1 and HS-5 stromal cells (1:1 ratio), as well as mono-cultured Ri-1 spheroids, were treated with DOX and IBR in triplicate at 6 concentrations between 0.001 and 100  $\mu$ M. Gels with spheroids were reincubated for 48 hours

after the addition of drugs. Next, the medium with drugs was gently aspirated, the spheroids were collected from the gel microwells and transferred into 96-well plates. A fresh cell culture medium with alamarBlue (Invitrogen, Germany) in an amount equal to 10% of the total volume was added and the plates were placed in an incubator for 24 h at 37 °C, protected from the light. The absorbance was then read at 570 nm and 630 nm using a spectrophotometer (BioTek Instruments, VT, USA). Cell proliferation was determined by calculating the percentage reduction of alamarBlue with the use of the alamarBlue Colorimetric Calculator provided by Bio-rad.<sup>46</sup> IC<sub>50</sub> values were derived by a sigmoidal dose-response (variable slope) curve using GraphPad Prism 9 software (GraphPad Software, San Diego, CA, USA).

## Anti-Cancer Drug Treatment with Doxorubicin Hydrochloride (DOX) and Ibrutinib (IBR)

Three-day co-cultures of Ri-1 and HS-5 stromal cells (1:1 ratio), as well as mono-cultured Ri-1 spheroids, were exposed to up to 0.05 and 0.5 µg/mL of DOX (Sigma-Aldrich, MO, USA) and 0.4 µmol/L of IBR (Sigma-Aldrich, MO, USA) for 48 h at 37 °C. Spheroids of the positive control for cytotoxicity were treated with 0.1% Triton-x-100 (TX) containing medium for 48 h. Untreated control spheroids were cultured in parallel. The proliferation/viability was assessed with an alamarBlue assay, as previously described.<sup>47</sup>

## Statistical Analysis

All data are represented as the mean ± standard deviation (SD). Statistical comparisons were performed using a one-way analysis of variance (ANOVA) followed by Student's *t*-test using Microsoft Excel 2018 (Microsoft Corp., CA, USA). *P*-values <0.05 were considered statistically significant.

## Results

### General Characteristics of B-NHL Spheroids

We developed hybrid models by co-culturing the representative B-NHL cell lines: Raji (BL) and Ri-1 (DLBCL) with MSCs in agarose hydrogels. Cells were plated at a density of 125 cells/well (in total  $3.2 \times 10^4$  cells per hydrogel), incubated for up to 14 days, followed by a visual assessment, image acquisition, and an analysis. Parallely, we researched the formation of self-assembled lymphoma aggregates followed by measurements of their overall morphology and size. Schematic illustrations of the 3D hybrid culture are presented in Figure 1A. In our model, stromal cells self-aggregate in the center of the spheroid and are evenly surrounded by layered lymphoma cells.

Different tumor and stromal cell ratios were prepared, including 1:1, 1:2, 1:4, and 1:10. Notably, in the case of ratios 1:4 and 1:10, we frequently observed the formation of multiple stromal spheroids within the individual wells. At the same time, we observed that co-culturing of lymphoma cells and MSCs in the ratio of 1:1 and 1:2 results in the best spheroid formation (Figure 1B); thus, further analyses were performed with a concentration ratio of 1:1. Next, we tried unsuccessfully to obtain the above model with the hanging drop method and the use of ultra-low attachment plates. As presented in Figure 1C, stromal cells aggregate in multiple, variable in size spheroids. In turn, lymphoma cells formed a flat, loose-structured, and irregularly shaped cell suspension. Notably, hydrogels allow forming a truly cohesive spheroid, not only a confined aggregated cell. Besides, this observation was further confirmed upon hematoxylin and immunohistochemical (IHC) staining (Figure 1D and E). B-NHL cells stained with an anti-CD20 monoclonal antibody are generally considered confirmatory of lymphoma cell infiltration into the BM, which is CD20 negative.

### Comparison of Morphology and Growth Rate of DLBCL and BL Spheroids

The dynamics of spheroids formation differed between the two B-NHL cell lines, as shown in Figure 2A. Raji cells, representing BL, developed a more compact and homogeneous in shape spheroids when compared to Ri-1 cells (DLBCL), which formed spheroids of apparently looser structure. Raji and Ri-1 cells aggregated in 24 h after seeding onto hydrogel microwells when co-cultured with MSCs and reported here timeline is comparable with the spheroid formation of other solid tumors. In turn, mono-cultured cells required three days to generate spheroids, which showed irregular shapes with a rough surface. Importantly, we observed that lymphoma cell aggregation into a 3D structure was

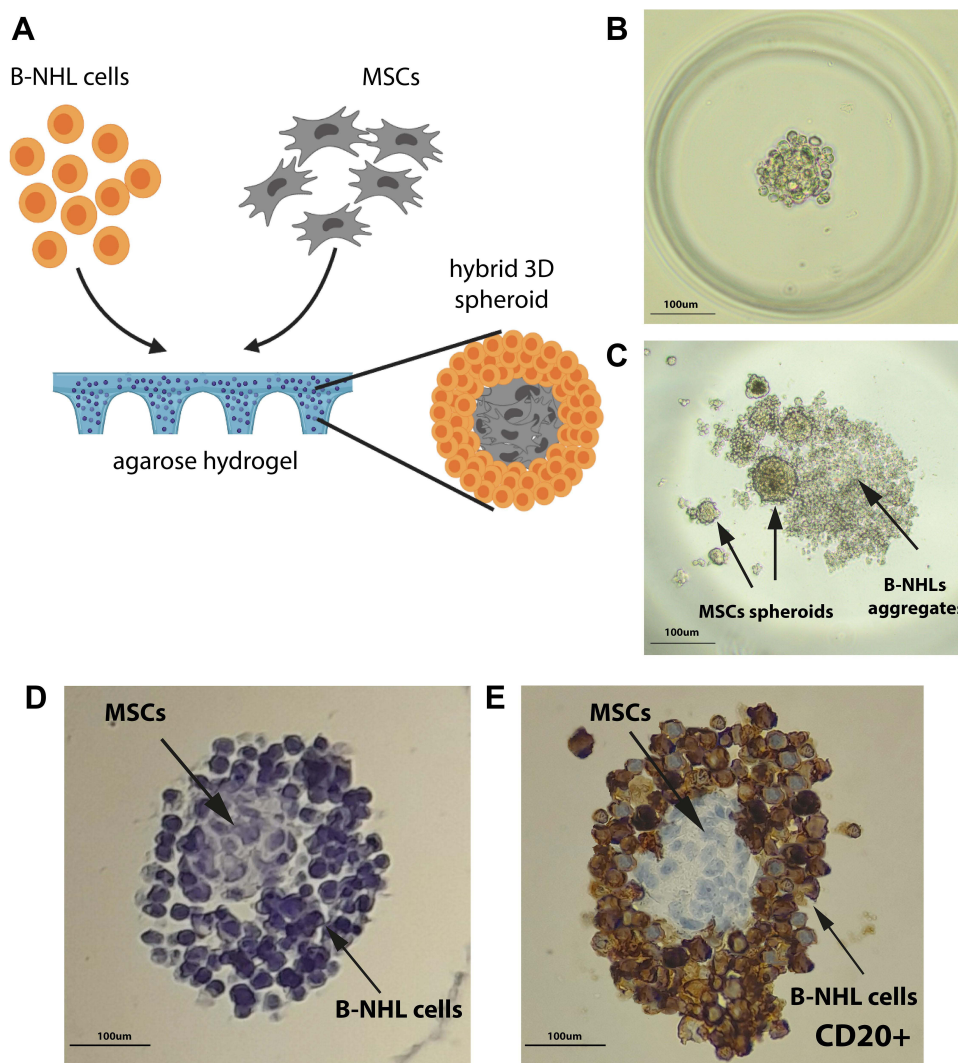


**Figure 1** Culture and staining of B-NHL spheroids. **(A)** Schematic illustration of the assembly of a 3D hybrid spheroid. Stromal cells (HS-5) aggregate densely, while lymphoma cells evenly surround the stromal cell core. **(B)** Lymphoma/MSCs hybrid spheroids (ratio 1:1) formed within agarose gel within 24 h. **(C)** Co-culture of HS-5 and Ri-1 cells in a “hanging drop” after 72 h of incubation. MSCs form multiple spheroids variable in size, while lymphoma cells are assembled into a flat, irregular aggregate. **(D)** Hematoxylin staining of FFPE spheroids (ratio 1:2 of Ri-1:HS-5) in agarose gel. **(E)** Immunohistochemical staining shows CD20 positive lymphoma cells surrounding the CD20 negative stromal cells, which self-aggregate in the center of the spheroid.

**Abbreviations:** B-NHL, B-cell non-Hodgkin lymphomas; 3D, three-dimensional; MSCs, mesenchymal stromal cells; FFPE, formalin-fixed paraffin-embedded.

significantly stimulated when co-cultured with MSCs for both cell lines. Mono-culturing of both lymphoma cell lines resulted in more loosely aggregated spheroids in comparison to co-culturing with MSCs. We observed that hybrid spheroids survived gentle handling without significant damage, unlike lymphoma mono-spheroids, which were easily dissociated by handling, suggesting low cell–cell adhesion.

Next, we revealed that the growth rates of mono- and co-cultured Raji spheroids were significantly faster than Ri-1 spheroids (Figure 2B and C). The highest proliferation of Raji spheroids was observed between days 3 and 5, while the most prominent increase of Ri-1 spheroids growth was noted between days 5–7 after seeding. After seven days of incubation, the average diameter of mono-cultured and co-cultured RAJI spheroids was  $369 \pm 69 \mu\text{m}$  and  $321 \pm 73 \mu\text{m}$ , respectively. In turn, mono- and co-cultured Ri-1 cells formed significantly smaller spheroids with a diameter of  $244 \pm 53 \mu\text{m}$ , and  $199 \pm 38 \mu\text{m}$ , respectively. The above data suggest that the growth of lymphoma spheroids was not stimulated when co-cultured with stromal cells; furthermore, a significantly lower diameter of the co-cultured spheroids was observed in comparison to mono-cultured spheroids.

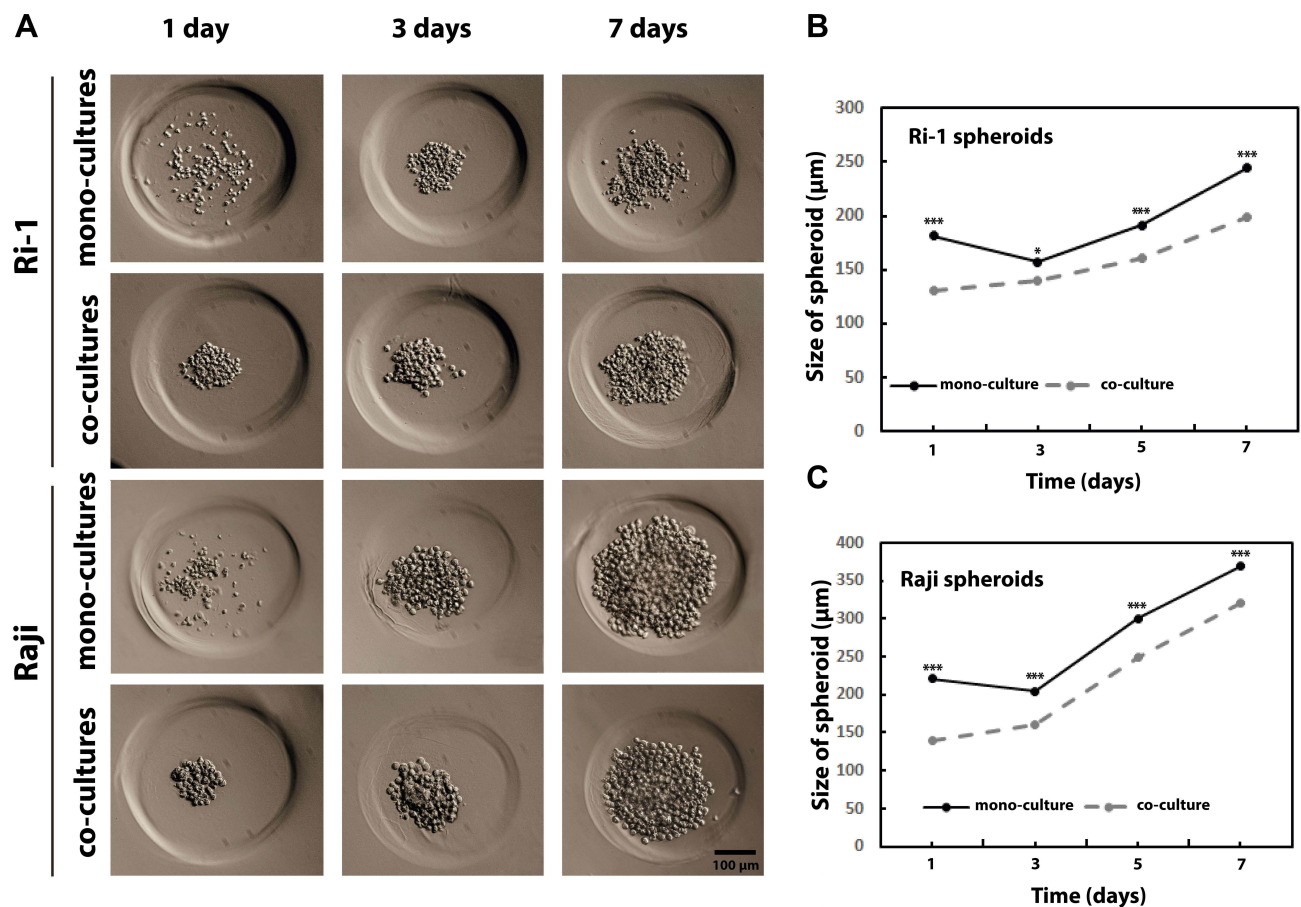


**Figure 2** The growth and morphology of Ri-1 (DLBCL) and RAJI (BL) spheroids over time. **(A)** Typical images of mono- and co-cultured spheroids. For both cell lines, co-cultured spheroids were formed within 24 h after seeding, while mono-cultured cells required 72 h to form the spheroids of an apparently looser structure. **(B and C)** Growth curves for Ri-1 and RAJI spheroids up to 7 days after seeding. The growth rates of mono- and co-cultured Raji spheroids were significantly faster than those of Ri-1 spheroids. The calculation of the diameter of spheroids was performed using bright field images and the Image J program. The measurements are presented as the mean  $\pm$  SD of 15 spheroids formed in three independent experiments. \* $P < 0.05$ , \*\*\* $P < 0.001$ .

**Abbreviations:** DLBCL, diffuse large B-cell lymphoma; BL, Burkitt Lymphoma; SD, standard deviation.

## Determination of the Viability of B-NHL Spheroids

Raji cells were mono-cultured or co-cultured with stromal cells followed by live/dead fluorescent staining and imaging of spheroids after 7 and 14 days. At the same time, the percentage of cell viability in Raji and Ri-1 spheroids was measured by the trypan blue dye exclusion method. Spheroids were resuspended in TrypLE Express before cell counting.

The live/dead cell assay results revealed that the viability of both: mono- and co-cultured cells during spheroid formation was preserved at seven days of incubation (Figure 3A). Calcein AM-stained green fluorescing viable cells made up the bulk of the spheroid, while the dead cells labeled with ethidium homodimer made up a small percentage of the spheroids. In turn, at the 14th day of incubation, a larger proportion of red fluorescent signal was observed, indicating significantly decreased viability of cells in the spheroids compared to the seventh day of co-culturing. Dead cells were evenly distributed throughout the mono- and co-cultured spheroid, and no region with prominent dead cell accumulation was detected. Moreover, the live/dead fluorescent staining revealed that mono-culturing of Ri-1 cells results in more loosely aggregated spheroids in comparison to co-culture with stromal cells. Importantly, cell survival was apparently higher in hybrid spheroids compared to mono-cultured spheroids (62.5 versus 47.8%), which may be due to the protective role of stromal cells (Figure 3B).

In line with the fluorescent staining results, after seven days of culturing, cell viability was 93% or greater for all lymphoma spheroids as confirmed by the results of the trypan blue exclusion assay (Figure 3C). In turn, cell viability assays on day 14 indicated a significant decrease in cells viability for all spheroids. Importantly, significant differences between the viability of mono- and co-cultured spheroids were revealed for both cell lines. This was particularly evident

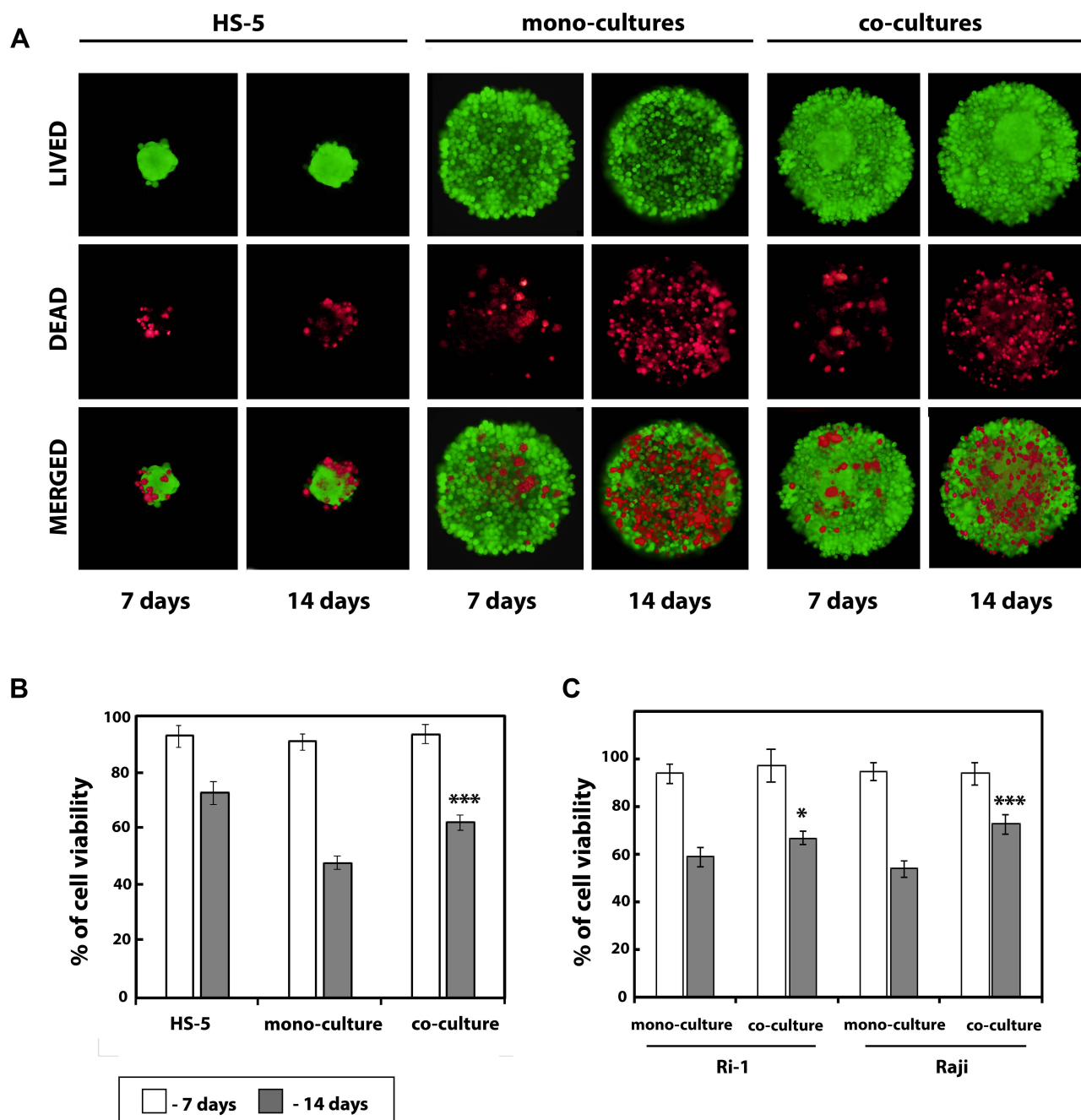


**Figure 3** B-NHL spheroids viability after a different period of culture. **(A)** Live/dead assay for the viability of the hybrid lymphoma/MSCs spheroids. Live/dead staining was performed on the 7th and 14th days of incubation. Green fluorescence indicates calcein AP stain in the live cells, and red fluorescence indicates the ethidium homodimer stain in the dead cells. **(B)** Quantification from the live/dead assay using ImageJ software. An index of live cells (% of cell viability) was constructed from the ratio of live to total cell numbers. **(C)** Percentage cell viability (viable cell count/total cell count) measured at days 7 and 14 using the trypan blue dye exclusion technique. Data from five independent experiments were analyzed and presented as the mean  $\pm$  SD. \* $P < 0.05$ , \*\*\* $P < 0.001$ , compared to mono-cultured cells. **Abbreviations:** B-NHL, B-cell non-Hodgkin lymphomas; MSCs, mesenchymal stromal cells.

in Raji spheroids, where mono-cultured cells were significantly less viable than co-cultured cells (54 versus 72%, respectively) while the viability of mono-cultured and co-cultured Ri-1 cells was 59% and 67%, respectively.

### Loss of Cell Proliferation

The  $IC_{50}$  values, defined as the half-inhibitory concentration were obtained for mono- and co-cultured Ri-1 spheroids by alamarBlue assay. There were no significant differences in the activity of doxorubicin between mono- and co-cultured spheroids ( $IC_{50}$  values of 0.833 and 0.72, respectively), **Figure 4A**, while ibrutinib was active at much lower doses on mono-cultured



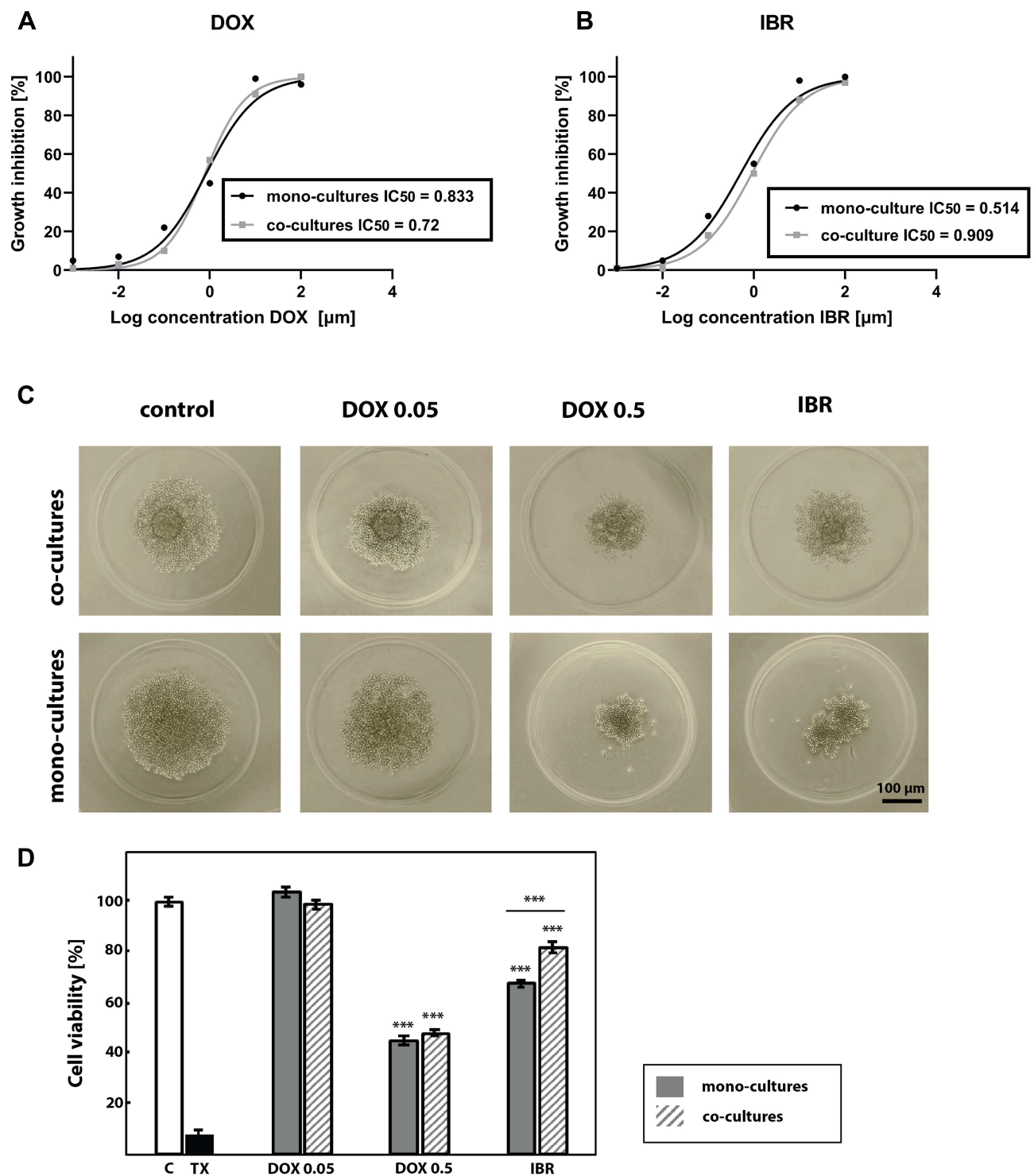


**Figure 4** Anti-cancer drug treatment of B-NHL hybrid spheroids. Growth inhibition and corresponding  $\text{IC}_{50}$  values of DOX (**A**) and IBR (**B**) in mono-cultured and co-cultured Ri-I spheroids as determined by alamarBlue assay. Mono-cultured and co-cultured spheroids were treated with the range of drug concentrations. Data points represent average of  $n=3$  experiments with eight technical replicates per DOX and IBR concentrations. (**C**) Light microscope images of Ri-I cell line untreated and treated with DOX and IBR at day 3 after treatment. (**D**) Cell viability of mono-cultured and co-cultured Ri-I spheroids under the anti-cancer treatment assessed by the use of the alamarBlue assay. Data were reported as the percentage of cell viability normalized to untreated control spheroids. Spheroids of the positive control for cytotoxicity were treated with 0.1% Triton-x-100 (TX).  $***P<0.001$ ; compared to control.  $***P<0.001$  underline; mono-culture versus co-culture.

**Abbreviations:** B-NHL, B-cell non-Hodgkin lymphomas; DOX, doxorubicin; IBR, ibrutinib, TX, Triton-X100.

spheroids ( $IC_{50}=0.514$ ) than co-cultured spheroids ( $IC_{50}=0.909$ ), **Figure 4B**. For anti-cancer treatment, the DOX doses were chosen such that they covered  $IC_{50}$  values. IBR dose was chosen within a maximum range equivalent to clinical concentration.

## Anti-Cancer Drug Treatment

We assessed the cell viability of the mono-cultured and co-cultured Ri-1 lymphoma spheroids under anti-cancer conditions: DOX (0.05 and 0.5  $\mu\text{g/mL}$ ) and IBR (0.4  $\mu\text{mol/L}$ ). Spheroids morphology presented in **Figure 4C** reflect the effect of drug treatment. No cytotoxic effects were observed when spheroids were treated with 0.05  $\mu\text{g/mL}$  of DOX for 72 h. Conversely, treatment with 0.5  $\mu\text{g/mL}$  of DOX for 72 h resulted in spheroid shrinkage and detachment of dead cells from the outer layers. No differences were observed between mono-cultured and co-cultured spheroids. In turn, a large decrease in the spheroid diameter was observed after the IBR treatment, particularly in mono-culturing cells. This is in line with experimental results determined by the alamarBlue assay (**Figure 4D**) revealing that cell viability was unaffected by 0.05  $\mu\text{g/mL}$  of DOX, while that 0.5  $\mu\text{g/mL}$  of DOX was significantly cytotoxic for mono- and co-cultured spheroids. No differences were observed between mono- and co-cultured cells (decrease in cell viability below 45% and 48%, respectively). In turn, our data revealed that mono-cultured cells were significantly more sensitive to IBR than co-cultures ( $P<0.001$ ).

## Discussion

In this work, we developed a 3D model for studying the crosstalk between B-NHL cells and BM stromal cells. Stromal cells are an essential component of the BM microenvironment that impacts tumor development and survival. Numerous works have described the stroma of the bone marrow as a “sanctuary site” for lymphoma cells during traditional immunochemotherapy, which significantly contributes to drug resistance and leads in consequences to therapy failure.<sup>48</sup> However, the reported antitumor effects are still controversial.<sup>49</sup> Current data suggest that MSCs may both promote and constrain tumor growth, although their net effect appears to be predominantly pro-tumorigenic.<sup>50</sup> There is mounting evidence that MSCs restrict tumor growth by suppressing angiogenesis, inhibiting proliferation-related signaling pathways like PI3K, Wnt, and AKT, and inhibiting cell cycle progression.<sup>51</sup> It was also suggested that MSCs appear to influence pathways that can suppress both proliferation and apoptosis.<sup>42,52,53</sup> Interestingly, both inhibitory and proliferative effects of MSCs have been reported in the same studies.<sup>54,55</sup> Discrepancies in the available data show that the biological role of BM stromal cells in cancer pathogenesis is not fully characterized. Meanwhile, it is believed that a better understanding of MSCs-tumor cells crosstalk will contribute to developing new treatment strategies in the future.<sup>56</sup> Several reports showed that stromal cells chemoprotect tumor cells through direct cell–cell contact; thus, there is an urgent need to develop models which allow studying such direct interactions.<sup>19</sup> Importantly, our group previously investigated the direct interactions between B-cell lymphoma and stromal cells in optical tweezers using a 2D culture,<sup>57,58</sup> whereas the 3D organization and cellular microenvironment emerged as critical determinants of lymphoma pathogenesis and drug resistance.

While 3D models of solid tumors are widely developed, the hemato-oncological malignancies remain omitted. Lymphocytes are generally mobile. B-lymphocytes within the lymph nodes remain in contact; however, they do not form solid cell structures. Similar to leukemias and myelomas, B-NHLs grow in a suspension when cultured in vitro, which results in difficulties in obtaining cohesive spheroids. The choice of a 3D culturing method is not without significance in the case of hemato-oncological malignancies such as B-NHLs. In the current study, we observed that B-NHL cells are grown within an ultra-low attachment plate or a hanging drop method aggregating into loose clumps of cells instead of 3D structures, which was previously described.<sup>59</sup> Such methods may be helpful in drug studies; however, they do not support cell–cell and microenvironment interactions. Here, we observed that the lymphoma cells form tight spheroids with agarose gel; however, the cells disintegrate when transferred with a pipette for further examination. Interestingly, when co-cultured with MSCs, B-NHL cells form compact and truly cohesive spheroids, which was previously described by Barboglio et al on the chronic lymphocytic leukemia (CLL) model.<sup>60</sup>

The HS-5 cell line used in this study was intentionally selected as HS-5 is a well-characterized model for the haemato-lymphopoietic microenvironment.<sup>20</sup> A genome-wide analysis has revealed a similarity in the transcriptional profile of human primary MSCs and HS-5 cell lines, indicating their relevance to MSCs-lymphoma interactions studies.<sup>61</sup>

A co-culture method with HS-5 stromal cells has been used successfully in previous reports to generate CLL<sup>60</sup> and multiple myeloma (MM) spheroids.<sup>62</sup> Co-culturing of stromal cells and MM cells led to the promotion of pro-survival signaling and cell adhesion-mediated drug resistance.<sup>62</sup> On the other hand, higher cell–cell interactions and better cell retention and homing inside the 3D leukemia model were observed when CLL cells were co-cultured with stromal cells.<sup>60</sup>

The size of spheroids is a critical factor that affects the transport of therapeutics through the tumor model; thus, it should ideally be controlled for application in drug evaluation studies. The spheroid size of 200–500 µm is recommended for flexibility and ease of handling for most applications.<sup>63</sup> The rationale is that smaller spheroids may not reproduce in vivo cell–cell and cell–microenvironment interactions. On the other hand, larger models may contain a hypoxic core that can affect cell behavior and alter interpretations of growth or survival assays. Notably, the size of our spheroids is compatible with a variety of adherent tumor and normal cell lines.<sup>63</sup> Additionally, we showed that when cultured to specific time points, the established hydrogel mono- and co-cultures effectively produce uniform in size lymphoma spheroids for subsequent studies.

In this work, lymphoma spheroids were successfully formalin-fixed and processed directly in the agarose hydrogel via automated tissue processing and paraffin embedding. Thus, we confirmed that using hydrogel microwells allows applying the standard procedure for histological tissue processing, including paraffin embedding and cutting without removing spheroids from hydrogels. This is especially challenging in the key hemato-oncological models and it often destroys the weak connections between cells. Surprisingly, when we further stained hybrid spheroids with hematoxylin, we observed the clearly layered structure, where stromal cells aggregate in the center of the spheroid and are evenly surrounded by lymphoma cells. The observed self-organization process might recapitulate the in vivo DLBCL–BM interactions.

Tumor-stromal interactions affect B-NHL cells' behavior, including survival and drug resistance. 3D cultures that recapitulate lymphoma–BM interactions are needed to thoroughly investigate disease progression and response to drugs, they are, however, unavailable. To evaluate the impact of BM stromal cells on doxorubicin (DOX) and ibrutinib (IBR) sensitivity, we performed parallel experiments in 3D mono-cultures versus 3D co-cultures using HS-5 stromal cells. The DOX<sup>64,65</sup> and IBR<sup>66,67</sup> concentrations were chosen within a range equivalent to clinical concentrations.

DOX is a chemotherapy medication used to treat cancer, including breast carcinoma, bladder carcinoma, Kaposi's sarcoma, lymphoma including B-NHLs, and acute lymphoblastic leukemia. DOX is the main cytotoxic component of the R-CHOP (rituximab, cyclophosphamide, *doxorubicin*, vincristine, prednisone) treatment regimen. DLBCLs include two major molecular subtypes; the germinal center B-cell-like (GCB) and the activated B-cell-like (ABC). DLBCL, represented in the Ri-1 cell line in this study, comes from ABC-DLBCL. It is well documented that ABC-DLBCL patients have poorer survival than GCB-DLBCLs under R-CHOP immunotherapy.<sup>68</sup>

In this work, we observed the high efficacy of DOX 0.5 µg/mL on mesenchymal stromal cells, both: when treated with a single drug or together with lymphoma cells. Interestingly, identical doses of DOX (0.05 and 0.5 µg/mL) were used in the canine 3D hybrid model of DLBCL by An et al, showing high efficacy at both tested doses.<sup>38</sup> Notably, in our study, no protective effect of MSCs in 3D DLBCL culture was observed, which is in line with the recent report of Lamaison et al performed on DLBCL and follicular lymphoma (FL) spheroids.<sup>69</sup> Importantly, hybrid models described here share other characteristics with DLBCL spheroids developed by Lamaison and co-authors. First, we observed a similar survival decrease during the second week of culture; however, the rate of cell death of our model was significantly lower. Next, Lamaison et al established that the survival decrease observed during the second week of culture is not associated with the formation of a hypoxic core, which is typically observed in 3D models of solid tumors. Accordingly, we did not detect any regionalization of dead cells deposition within the spheroid. Finally, the authors confirmed a supportive role of stromal cells (lymphoid stromal cells isolated from tonsils) in B-NHL spheroid formation.

Another important drug for the clinical treatment of DLBCL is ibrutinib. IBR is an oral irreversible inhibitor of Bruton's tyrosine kinase (BTK), which performs a critical role in the oncogenic signal transduction pathway downstream of the B-cell antigen receptor in various B-NHLs, including CLL, mantle cell lymphoma (MCL), and Waldenström's macroglobulinemia.<sup>70</sup> Currently, IBR is thought to be a promising target drug of DLBCL, especially several clinical trials showed the potential to improve tumor response of patients with ABC-DLBCL. In this study, we evidenced that IBR

more significantly affects ABC-DLBCL spheroids in the absence of BM-derived stromal cells, indicating a protective role exerted by the microenvironment, possibly through a direct contact with BM-derived stromal cells. This is further supported by the significantly greater drug resistance observed in 3D hybrid models compared to what was previously observed in spheroid mono-cultures.<sup>68,71</sup> This creates the possibility that a similar environment may exist in the DLBCL environment in vivo. The above results indicate that tumor microenvironment (TME), tissue tension and adhesion are essential factors affecting lymphoma cell susceptibility to treatment.<sup>72,73</sup> Moreover, these results suggest that our 3D hybrid model recapitulates the variability of drug response among B-NHLs.

## Conclusion

The 3D co-culture, where lymphoma cells interact with stromal components, is particularly important in developing a more clinically relevant model. Such a model should be monitored through time and applied in studying the lymphoma response to various therapies. Here, we established and described cheap and fast hydrogel-based 3D co-cultures that can be used in a wide range of applications, including cell signaling or candidate drug screening. We believe that the above model may be necessary to develop a personalized therapy for patients with recurrent or refractory lymphoma with BM involvement.

## Abbreviations

ABC, activated B-cell-like; BAFF, B cell-activating factor belonging to the TNF family; B-NHLs, B-cell non-Hodgkin lymphomas; BM, bone marrow; BTK, Bruton's tyrosine kinase; BL, Burkitt lymphoma; CAF, cancer-associated fibroblasts; CLL, chronic lymphocytic leukemia; CTCF, corrected total cell fluorescence; DLBCL, diffuse large B-cell lymphoma; DMSO, dimethyl sulfoxide; DOX, doxorubicin; FL, follicular lymphoma; FFPE, formalin fixation and paraffin embedding; GCB, germinal center B-cell-like; IBR, ibrutinib; MCL, mantle cell lymphoma; MSCs, mesenchymal stromal cells; MM, multiple myeloma; THRLBCL, T-cell/histiocyte-rich large B-cell lymphoma, TAM, tumor-associated macrophages; TX, Triton-X100; 2D, two-dimensional; 3D, three-dimensional.

## Acknowledgments

The authors of this study would like to thank Piotr Ziółkowski from the Department of Clinical and Experimental Pathology, Wrocław Medical University for the mentoring support. K.D-S is grateful to Stanisława Nowak for continuous support and inspiration.

## Funding

This research was funded by The National Science Centre Poland (NCN, Poland); OPUS. UMO-2017/27/B/ST7/01255.

## Disclosure

The authors report no conflicts of interest in this work.

---

## References

1. Swerdlow SH, Campo E, Pileri SA, et al. The 2016 revision of the World Health Organization classification of lymphoid neoplasms. *Blood*. 2016;127(20):2375–2390. doi:10.1182/blood-2016-01-643569
2. Said JW. Aggressive B-cell lymphomas: how many categories do we need? *Mod Pathol*. 2013;26 Suppl 1(01):S42–S56. doi:10.1038/modpathol.2012.178
3. Campbell J, Seymour JF, Matthews J, et al. The prognostic impact of bone marrow involvement in patients with diffuse large cell lymphoma varies according to the degree of infiltration and presence of discordant marrow involvement. *Eur J Haematol*. 2006;76(6):473–480. doi:10.1111/j.1600-0609.2006.00644.x
4. Chung R, Lai R, Wei P, et al. Concordant but not discordant bone marrow involvement in diffuse large B-cell lymphoma predicts a poor clinical outcome independent of the International Prognostic Index. *Blood*. 2007;110(4):1278–1282. doi:10.1182/blood-2007-01-070300
5. Yao Z, Deng L, Xu-Monette ZY, et al. Concordant bone marrow involvement of diffuse large B-cell lymphoma represents a distinct clinical and biological entity in the era of immunotherapy. *Leukemia*. 2018;32(2):353–363. doi:10.1038/leu.2017.222
6. Crippa S, Santi L, Bosotti R, et al. Bone marrow-derived mesenchymal stromal cells: a novel target to optimize hematopoietic stem cell transplantation protocols in hematological malignancies and rare genetic disorders. *J Clin Med*. 2019;9(1):2. doi:10.3390/jcm9010002

7. Méndez-Ferrer S, Michurina TV, Ferraro F, et al. Mesenchymal and haematopoietic stem cells form a unique bone marrow niche. *Nature*. 2012;466(7308):829–834. doi:10.1038/nature09262
8. Kidd S, Caldwell L, Dietrich M, et al. Mesenchymal stromal cells alone or expressing interferon- $\beta$  suppress pancreatic tumors in vivo, an effect countered by anti-inflammatory treatment. *Cytotherapy*. 2011;13:498.
9. He N, Kong Y, Lei X, et al. MSCs inhibit tumor progression and enhance radiosensitivity of breast cancer cells by down-regulating Stat3 signaling pathway. *Cell Death Dis*. 2018;9(10):1026. doi:10.1038/s41419-018-0949-3
10. De Araújo Farias V, O'Valle F, Lerma BA, et al. Human mesenchymal stem cells enhance the systemic effects of radiotherapy. *Oncotarget*. 2015;6(31):31164–31180. doi:10.18632/oncotarget.5216
11. Otsu K, Das S, Houser SD, et al. Concentration-dependent inhibition of angiogenesis by mesenchymal stem cells. *Blood*. 2009;113(18):4197–4205. doi:10.1182/blood-2008-09-176198
12. Dasari VR, Velpula KK, Kaur K, et al. Cord blood stem cell-mediated induction of apoptosis in glioma downregulates X-linked inhibitor of apoptosis protein (XIAP). *PLoS One*. 2010;5(7):e11813. doi:10.1371/journal.pone.0011813
13. Suzuki K, Sun R, Origuchi M, et al. Mesenchymal stromal cells promote tumor growth through the enhancement of neovascularization. *Mol Med*. 2011;17(7–8):579–587. doi:10.2119/molmed.2010.00157
14. Karnoub AE, Dash AB, Vo AP, et al. Mesenchymal stem cells within tumour stroma promote breast cancer metastasis. *Nature*. 2007;449(7162):557–563. doi:10.1038/nature06188
15. Bussard KM, Mutkus L, Stumpf K, et al. Tumor-associated stromal cells as key contributors to the tumor microenvironment. *Breast Cancer Res*. 2016;18(1):84. doi:10.1186/s13058-016-0740-2
16. Le Naour A, Prat M, Thibault B, et al. Tumor cells educate mesenchymal stromal cells to release chemoprotective and immunomodulatory factors. *J Mol Cell Biol*. 2020;12(3):202–215. doi:10.1093/jmcb/mjz090
17. Hussain S, Peng B, Cherian M, et al. The roles of stroma-derived chemokine in different stages of cancer metastases. *Front Immunol*. 2020;11:598532. doi:10.3389/fimmu.2020.598532
18. Hill BS, Sarnella A, D'Avino G, et al. Recruitment of stromal cells into tumour microenvironment promote the metastatic spread of breast cancer. *Semin Cancer Biol*. 2020;60:202–213. doi:10.1016/j.semcancer.2019.07.028
19. Kumar A, Bhattacharyya J, Jagannathan BG. Adhesion to stromal cells mediates imatinib resistance in chronic myeloid leukemia through ERK and BMP signaling pathways. *Sci Rep*. 2017;7(1):9535. doi:10.1038/s41598-017-10373-3
20. Mraz M, Zent CS, Church AK, et al. Bone marrow stromal cells protect lymphoma B-cells from rituximab-induced apoptosis and targeting integrin  $\alpha$ -4- $\beta$ -1 (VLA-4) with natalizumab can overcome this resistance. *Br J Haematol*. 2011;155(1):53–64. doi:10.1111/j.1365-2141.2011.08794.x
21. Janssens R, Struyf S, Proost P. The unique structural and functional features of CXCL12. *Cell Mol Immunol*. 2018;15(4):299–311. doi:10.1038/cmi.2017.107
22. Lwin T, Crespo LA, Wu A, et al. Lymphoma cell adhesion-induced expression of B cell-activating factor of the TNF family in bone marrow stromal cells protects non-Hodgkin's B lymphoma cells from apoptosis. *Leukemia*. 2009;23(1):170–177. doi:10.1038/leu.2008.266
23. Breslin S, O'Driscoll L. Three-dimensional cell culture: the missing link in drug discovery. *Drug Discov Today*. 2013;18(5–6):240–249. doi:10.1016/j.drudis.2012.10.003
24. Edmondson R, Broglie JJ, Adcock AF, et al. Three-dimensional cell culture systems and their applications in drug discovery and cell-based biosensors. *Assay Drug Dev Technol*. 2014;12(4):207–218. doi:10.1089/adt.2014.573
25. Zoetemelk M, Rausch M, Colin DJ, et al. Short-term 3D culture systems of various complexity for treatment optimization of colorectal carcinoma. *Sci Rep*. 2019;9:7103.
26. Powley IR, Patel M, Miles G, et al. Patient-derived explants (PDEs) as a powerful preclinical platform for anti-cancer drug and biomarker discovery. *Br J Cancer*. 2020;122(6):735–744. doi:10.1038/s41416-019-0672-6
27. Unger FT, Witte I, David KA. Prediction of individual response to anticancer therapy: historical and future perspectives. *Cell Mol Life Sci*. 2015;72(4):729–757. doi:10.1007/s00018-014-1772-3
28. Imamura Y, Mukohara T, Shimono Y, et al. Comparison of 2D- and 3D-culture models as drug-testing platforms in breast cancer. *Oncol Rep*. 2015;33(4):1837–1843. doi:10.3892/or.2015.3767
29. Tung YC, Hsiao AY, Allen SG, et al. High-throughput 3D spheroid culture and drug testing using a 384 hanging drop array. *Analyst*. 2011;136(3):473–478. doi:10.1039/C0AN00609B
30. Benelli R, Zocchi MR, Poggi A. Three-Dimensional (3D) culture models in cancer investigation, drug testing and immune response evaluation. *Int J Mol Sci*. 2020;22(1):150. doi:10.3390/ijms22010150
31. Brüningk SC, Rivens I, Box C, et al. 3D tumour spheroids for the prediction of the effects of radiation and hyperthermia treatments. *Sci Rep*. 2020;10(1):1653. doi:10.1038/s41598-020-58569-4
32. Luca AC, Mersch S, Deenen R, et al. Impact of the 3D microenvironment on phenotype, gene expression, and EGFR inhibition of colorectal cancer cell lines. *PLoS One*. 2013;8(3):e59689. doi:10.1371/journal.pone.0059689
33. Goers L, Freemont P, Polizzi KM. Co-culture systems and technologies: taking synthetic biology to the next level. *J R Soc Interface*. 2014;11(96):20140065. doi:10.1098/rsif.2014.0065
34. Vis MAM, Ito K, Hofmann S. Impact of culture medium on cellular interactions in in vitro co-culture systems. *Front Bioeng Biotechnol*. 2020;8:911. doi:10.3389/fbioe.2020.00911
35. Mannino RG, Santiago-Miranda AN, Pradhan P, et al. 3D microvascular model recapitulates the diffuse large B-cell lymphoma tumor microenvironment in vitro. *Lab Chip*. 2017;17(3):407–414. doi:10.1039/C6LC01204C
36. Foxall R, Narang P, Glaysher B, et al. Developing a 3D B cell lymphoma culture system to model antibody therapy. *Front Immunol*. 2021;11:605231. doi:10.3389/fimmu.2020.605231
37. An JH, Song WJ, Li Q, et al. 3D-culture models as drug-testing platforms in canine lymphoma and their cross talk with lymph node-derived stromal cells. *J Vet Sci*. 2021;22(3):e25. doi:10.4142/jvs.2021.22.e25
38. Białkowska K, Komorowski P, Bryszewska M, et al. Spheroids as a type of three-dimensional cell cultures-examples of methods of preparation and the most important application. *Int J Mol Sci*. 2020;21(17):6225. doi:10.3390/ijms21176225
39. LaBarbera DV, Reid BG, Yoo BH. The multicellular tumor spheroid model for high throughput cancer drug discovery. *Expert Opin Drug Discov*. 2012;7(9):819–830. doi:10.1517/17460441.2012.708334

40. Monjaret F, Fernandes M, Duchemin-Pelletier E, et al. Fully automated one-step production of functional 3D tumor spheroids for high-content screening. *J Lab Autom.* 2016;21(2):268–280. doi:10.1177/2211068215607058
41. Caliarì SR, Burdick JA. A practical guide to hydrogels for cell culture. *Nat Methods.* 2016;13(5):405–414. doi:10.1038/nmeth.3839
42. Lee JM, Park DY, Yang L, et al. Generation of uniform-sized multicellular tumor spheroids using hydrogel microwells for advanced drug screening. *Sci Rep.* 2018;8(1):17145. doi:10.1038/s41598-018-35216-7
43. Lutolf MP, Hubbell JA. Synthetic biomaterials as instructive extracellular microenvironments for morphogenesis in tissue engineering. *Nat Biotechnol.* 2005;23(1):47–55. doi:10.1038/nbt1055
44. Tibbitt MW, Anseth KS. Hydrogels as extracellular matrix mimics for 3D cell culture. *Biotechnol Bioeng.* 2009;103(4):655–663. doi:10.1002/bit.22361
45. Determining fluorescence intensity and signal. University of Maryland, Baltimore County. Available from: <https://kpif.umbc.edu/image-processing-resources/imagej-fiji/determining-fluorescence-intensity-and-positive-signal/>. Accessed December 21, 2021.
46. Bio-Rad colorimetric and fluorometric calculator. Available from: <https://www.bio-rad-antibodies.com/colorimetric-calculator-fluorometric-alamarblue.html>. Accessed December 21, 2021.
47. Eilenberger C, Kratz SRA, Rothbauer M, et al. Optimized alamarBlue assay protocol for drug dose-response determination of 3D tumor spheroids. *MethodsX.* 2018;5:781–787. doi:10.1016/j.mex.2018.07.011
48. Meads MB, Hazlehurst LA, Dalton WS. The bone marrow microenvironment as a tumor sanctuary and contributor to drug resistance. *Clin Cancer Res.* 2008;14(9):2519–2526. doi:10.1158/1078-0432.CCR-07-2223
49. Lee MW, Ryu S, Kim DS, et al. Mesenchymal stem cells in suppression or progression of hematologic malignancy: current status and challenges. *Leukemia.* 2019;33(3):597–611. doi:10.1038/s41375-018-0373-9
50. Galland S, Stamenkovic I. Mesenchymal stromal cells in cancer: a review of their immunomodulatory functions and dual effects on tumor progression. *J Pathol.* 2020;250(5):555–572. doi:10.1002/path.5357
51. Liang W, Chen X, Zhang S, et al. Mesenchymal stem cells as a double-edged sword in tumor growth: focusing on MSC-derived cytokines. *Cell Mol Biol Lett.* 2021;26(1):3. doi:10.1186/s11658-020-00246-5
52. Wu YL, Li HY, Zhao XP, et al. Mesenchymal stem cell-derived CCN2 promotes the proliferation, migration and invasion of human tongue squamous cell carcinoma cells. *Cancer Sci.* 2017;108(5):897–909. doi:10.1111/cas.13202
53. Yulyana Y, Ho IA, Sia KC, et al. Paracrine factors of human fetal MSCs inhibit liver cancer growth through reduced activation of IGF-1R/PI3K/Akt signaling. *Mol Ther.* 2015;23(4):746–756. doi:10.1038/mt.2015.13
54. Klopp AH, Gupta A, Spaeth E, et al. Concise review: dissecting a discrepancy in the literature: do mesenchymal stem cells support or suppress tumor growth? *Stem Cells.* 2011;29(1):11–19. doi:10.1002/stem.559
55. Li L, Tian H, Yue W, et al. Human mesenchymal stem cells play a dual role on tumor cell growth in vitro and in vivo. *J Cell Physiol.* 2011;226(7):1860–1867. doi:10.1002/jcp.22511
56. Wang Q, Li T, Wu W, et al. Interplay between mesenchymal stem cell and tumor and potential application. *Hum Cell.* 2020;33(3):444–458. doi:10.1007/s13577-020-00369-z
57. Duś-Szachniewicz K, Drobczyński S, Woźniak M, et al. Differentiation of single lymphoma primary cells and normal B-cells based on their adhesion to mesenchymal stromal cells in optical tweezers. *Sci Rep.* 2019;9(1):9885. doi:10.1038/s41598-019-46086-y
58. Duś-Szachniewicz K, Drobczyński S, Ziółkowski P, et al. Physiological Hypoxia (Physioxia) impairs the early adhesion of single lymphoma cell to marrow stromal cell and extracellular matrix. *Optical Tweezers Study.* *Int J Mol Sci.* 2018;19(7):1880. doi:10.3390/ijms19071880
59. Gava F, Faria C, Gravelle P, et al. 3D model characterization by 2D and 3D imaging in t(14;18)-positive B-NHL: perspectives for in vitro drug screens in follicular lymphoma. *Cancers.* 2021;13(7):1490. doi:10.3390/cancers13071490
60. Barbaglio F, Belloni D, Scarfò L, et al. Three-dimensional co-culture model of chronic lymphocytic leukemia bone marrow microenvironment predicts patient-specific response to mobilizing agents. *Haematologica.* 2021;106(9):2334–2344. doi:10.3324/haematol.2020.248112
61. Adamo A, Delfino P, Gatti A, et al. HS-5 and HS-27A stromal cell lines to study bone marrow mesenchymal stromal cell-mediated support to cancer development. *Front Cell Dev Biol.* 2020;8:584232. doi:10.3389/fcell.2020.584232
62. Belloni D, Heltai S, Ponzoni M, et al. Modeling multiple myeloma-bone marrow interactions and response to drugs in a 3D surrogate microenvironment. *Haematologica.* 2018;103(4):707–716. doi:10.3324/haematol.2017.167486
63. Maritan SM, Lian EY, Mulligan LM. An efficient and flexible cell aggregation method for 3D spheroid production. *J Vis Exp.* 2017;121:55544.
64. McHowat J, Swift LM, Arutunyan A, et al. Clinical concentrations of doxorubicin inhibit activity of myocardial membrane-associated, calcium-independent phospholipase A(2). *Cancer Res.* 2001;61(10):4024–4029.
65. Xu P, Zuo H, Chen B, et al. Doxorubicin-loaded platelets as a smart drug delivery system: an improved therapy for lymphoma. *Sci Rep.* 2017;7(1):42632. Erratum in: *Sci Rep.* 2017;7:44974. doi:10.1038/srep42632
66. Ma J, Lu P, Guo A. Characterization of ibrutinib-sensitive and -resistant mantle lymphoma cells. *Br J Haematol.* 2014;166(6):849–861. doi:10.1111/bjh.12974
67. Wu W, Wang W, Franzen CA, et al. Inhibition of B-cell receptor signaling disrupts cell adhesion in mantle cell lymphoma via RAC2. *Blood Adv.* 2021;5(1):185–197. doi:10.1182/bloodadvances.2020001665
68. Mai Y, Yu JJ, Bartholdy B, et al. An oxidative stress-based mechanism of doxorubicin cytotoxicity suggests new therapeutic strategies in ABC-DLBCL. *Blood.* 2016;128(24):2797–2807. doi:10.1182/blood-2016-03-705814
69. Lamaison C, Latour S, Hélaine N, et al. A novel 3D culture model recapitulates primary FL B-cell features and promotes their survival. *Blood Adv.* 2021;5(23):5372–5386. doi:10.1182/bloodadvances.2020003949
70. Hou K, Yu Z, Jia Y, et al. Efficacy and safety of ibrutinib in diffuse large B-cell lymphoma: a single-arm meta-analysis. *Crit Rev Oncol Hematol.* 2020;152:103010. doi:10.1016/j.critrevonc.2020.103010
71. Bray LJ, Binner M, Körner Y, et al. A three-dimensional ex vivo tri-culture model mimics cell-cell interactions between acute myeloid leukemia and the vascular niche. *Haematologica.* 2017;102:1215–1226. doi:10.3324/haematol.2016.157883
72. Khawar IA, Park JK, Jung ES, et al. Three dimensional mixed-cell spheroids mimic stroma-mediated chemoresistance and invasive migration in hepatocellular carcinoma. *Neoplasia.* 2018;20(8):800–812. doi:10.1016/j.neo.2018.05.008
73. Yip D, Cho CH. A multicellular 3D heterospheroid model of liver tumor and stromal cells in collagen gel for anti-cancer drug testing. *Biochem Biophys Res Commun.* 2013;433(3):327–332. doi:10.1016/j.bbrc.2013.03.008

OncoTargets and Therapy

Dovepress

### Publish your work in this journal

OncoTargets and Therapy is an international, peer-reviewed, open access journal focusing on the pathological basis of all cancers, potential targets for therapy and treatment protocols employed to improve the management of cancer patients. The journal also focuses on the impact of management programs and new therapeutic agents and protocols on patient perspectives such as quality of life, adherence and satisfaction. The manuscript management system is completely online and includes a very quick and fair peer-review system, which is all easy to use. Visit <http://www.dovepress.com/testimonials.php> to read real quotes from published authors.

Submit your manuscript here: <https://www.dovepress.com/oncotargets-and-therapy-journal>